UDC 629.78.03: 621.472

Doi: 10.31772/2712-8970-2025-26-3-408-430

**Для цитирования:** Финогенов С. Л., Коломенцев А. И., Назаров В. П. Полетная эффективность солнечного теплового ракетного двигателя с двухступечатым тепловым аккумулятором // Сибирский аэрокосмический журнал. 2025. Т. 26, № 3. С. 408–430. Doi: 10.31772/2712-8970-2025-26-3-408-430.

**For citation:** Finogenov S. L., Kolomentsev A. I., Nazarov V. P. [Flight efficiency of solar thermal propulsion with double-stage thermal energy storage]. *Siberian Aerospace Journal.* 2025, Vol. 26, No. 3, P. 408–430. Doi: 10.31772/2712-8970-2025-26-3-408-430.

# Полетная эффективность солнечного теплового ракетного двигателя с двухступечатым тепловым аккумулятором

С. Л. Финогенов $^{1*}$ , А. И. Коломенцев $^{1}$ , В. П. Назаров $^{2}$ 

<sup>1</sup>Московский авиационный институт (национальный исследовательский университет) Российская Федерация, 125993, г. Москва, Волоколамское шоссе, 4 <sup>2</sup>Сибирский государственный университет науки и технологий имени академика М. Ф. Решетнева Российская Федерация, 660037, г. Красноярск, просп. им. газ. «Красноярский рабочий», 31 \*E-mail: sfmai2015@mail.ru

Аннотация. Актуальность работы связана с возрастающей потребностью в тяжелых спутниках на высоких рабочих орбитах. Рассматриваемый в работе солнечный тепловой ракетный двигатель (СТРД) с двухступенчатым фазопереходным тепловым аккумулятором (ТА) предназначен для выведения космического аппарата (КА) на геостационарную орбиту (ГСО). Двухступенчатый TA включает внешнюю низкотемпературную ступень системы «солнечный концентраторсветоприемник-аккумулятор» (КПА), содержащую энергоемкий фазопереходный теплоаккумулирующий материал (ТАМ) с относительно невысокой температурой плавления, типа гидрида лития, и высокотемпературную центральную ступень с тугоплавким энергоемким ТАМ, например, оксидом бериллия, что обеспечивает высокий удельный импульс двигателя 900 с. Время межорбитального перелета варьируется от 20 до 90 суток. Выявленные рациональные оптикоэнергетические параметры двигателя в этом диапазоне определяют требуемую точность солнечного концентратора, более низкую по сравнению с одноступенчатой системой КПА, поэтому условия слежения за Солнцем в полете могут быть значительно упрощены. Сравнение характеристик СТРД с альтернативными средствами межорбитальной транспортировки показывает, что энергобаллистическая эффективность КА в рассматриваемой задаче значительно превосходит таковую для химических или комбинированных космических разгонных блоков с электроракетным довыведением на ГСО. Использование двигателя с дожиганием нагретого в ТА водорода кислородом позволяет повысить полезную массу на ГСО при сравнительно небольшом времени перелета и сократить размеры КА с СТРД. Целесообразные величины соотношения расходов компонентов топлива зависят от времени перелета. Рассмотренные возможные варианты полезной нагрузки – геостационарных спутников связи – могут быть выведены на целевую орбиту при помощи ракетыносителя среднего класса «Союз-2.1б» с «солнечным» разгонным блоком вместо тяжелых носителей типа «Протон-М» с химическими верхними ступенями.

Ключевые слова: солнечный тепловой ракетный двигатель, ступени нагрева водорода, тепловой аккумулятор, геостационарная орбита, космический аппарат.

# Flight efficiency of solar thermal propulsion with double-stage thermal energy storage

S. L. Finogenov<sup>1\*</sup>, A. I. Kolomentsev<sup>1</sup>, V. P. Nazarov<sup>2</sup>

<sup>1</sup>Moscow Aviation Institute (National Research University)
 4, Volokolamskoe shosse, Moscow, 125993, Russian Federation
 <sup>2</sup>Reshetnev Siberian State University of Science and Technology
 31, Krasnoyarskii rabochii prospekt, Krasnoyarsk, 660037, Russian Federation
 \*E-mail: sfmai2015@mail.ru

Abstract. The activity urgency is connected with requirement of heavy spacecraft ascent into high working orbits. The solar thermal propulsion (STP) with double-stage latent heat thermal energy storage (TES) is intended for space vehicle delivery into geostationary orbit (GEO). Double-stage TES contains peripheral stage as "solar concentrator – sunlight absorber-thermal energy storage" system (CATS) with relatively low-temperature heat-accumulating phase-changing material (HAM) having high latent heat of fusion, for instance, lithium hydride, and high-temperature central stage with high power-intensive TES, for example, beryllium oxide, that allows to obtain high specific impulse 900 sec. Inter-orbital transfer time from low earth orbit (LEO)-to-GEO varies from 20 to 90 days. Expedient optical-energetic characteristic parameters of the STRE for each flight time shows that expedient accuracy of the solar mirror concentrator is much less in comparison with single-stage CATS with beryllium oxide as the HAM, therefore, the CATS Sun tracking conditions can be significantly simplified. Comparison between the STRE and alternative means of inter-orbital transportation shows that payload mass on GEO seriously exceeds that for liquid propulsion or combined upper stages with both chemical and electric propulsion. Use of the STRE with heated hydrogen after-burning allows payload mass to increase at relatively low transfer time, as well as reduce space vehicle dimensions and the CATS complication. The expedient oxidizer-to-fuel mass ratios depend on LEO-to-GEO trip time. The considered possible variants of payloads – geostationary communication satellites - can be injected into the target orbit with use of "Soyuz-2.1b" middle class launchers having the "solar" upper stage instead of "Proton-M" heavy rockets class with chemical liquid-propellant kick-stages.

Keywords: solar thermal propulsion, stages of hydrogen heating, thermal energy storage, geostationary orbit, hydrogen after-burning.

### Introduction

The significance of the research is determined by the need of modern cosmonautics for new means of interorbital transportation to high-energy working orbits, including the geostationary orbit (GEO). Since the capabilities of chemical rocket engines (LPRE and SRE) are reaching their limits, and propilsion with a high specific impulse (NRP, ERP) have limitations in their use, it is relevant to use the energy of the external environment of outer space, in particular, solar energy, as the most accessible for increasing the enthalpy of rocket fuel. In this concern, it is advisable to develop a solar thermal propulsion (STP) with direct heating of the working fluid (hydrogen) in the "solar concentrator – solar radiation receiver" (CATS) system. The STP is characterized by a fairly high specific impulse (up to 800–900 s) and a jet thrust in the range of 100–1000 N, which allows it to be classified as an "intermediate" thrust engine compared to liquid rocket engines and electric rocket engines.

The level of such "intermediate" thrust of a spacecraft (SC) with a STP assumes multiple "discontinuous" trajectories with active sections in the apsidal regions of transition trajectories with passive movement between them. First, perigee engine firings are performed with a tangential direction of the jet thrust vector, and then, after reaching the apogee region of the geostationary transfer orbit, or higher, apogee tangential engine firings are performed with control, including by the yaw angle, to change the orbital inclination and round it to the GEO level.

During the flight along the passive trajectory sections, it is advisable to use a thermal accumulator (TA) to accumulate thermal energy from the solar concentrator to use it to heat the working fluid (hydrogen) in the active orbit sections and to create thrust for the sequential raising of the orbit and changing its inclination [1; 2]. Therefore, the advantage of the STP with TA is the independence of the energy accumulation processes when the engine does not operate in the passive sections of the trajectory and the simplification of the conditions for orienting the "solar concentrator – sunlight absorber-thermal energy storage" (CATS) system to the Sun, and turning on the engine in the active sections, regardless of the shading conditions of the apsidal line. There could be used solid materials such as siliconized graphite, which accumulate heat due to heat capacity [2; 3], and heat-accumulating phase-changing materials, which have a high specific latent heat of fusion and do not change the energy output at the outlet of the heat storage material (HSM) during the entire duration of the thermal discharge [4; 5]. In the future, we will consider phase-transition materials as having high specific energy capacity and prospects for further improvement of their application, in particular, the possibility of using superheated HAM in combination with a solid matrix [3].

#### Two-stage CATS system

Previously, the research [6–8] considered STRE with single-stage phase-change TES, the possibility of using various heat-accumulating materials was assessed. The disadvantage of single-stage light receiver-accumulators is their isothermal nature, since the entire beam-absorbing surface can be considered as an absolutely black body, emitting uniformly across the entire diameter of the aperture of the radial-type light receiver-accumulator in the range of wavelengths corresponding to the maximum heating temperature, which inevitably reduces the CATS efficiency and requires high precision of the mirror surface of the solar concentrator and its orientation to the Sun.

We could assume a normal (Gaussian) distribution of the radiant flux in the focal light spot, which is quite consistent with the experimental aberrograms of real paraboloid mirrors [9; 10]. In this case, it can be concluded that it is possible to create a two-stage TES with a first (low-temperature) peripheral annular stage made on the basis of a not too heat-proof HAM with a high latent heat of melting, such as lithium hydride LiH, and the second (high-temperature) central stage containing, for example, beryllium oxide BeO. The choice of beryllium oxide as a high-temperature propellant (HAM) is due to its high energy capacity and high melting point with the possibility of heating hydrogen to high temperatures of about 2800 K, which ensures a high specific impulse of the engine thrust, reaching 900 s when using hydrogen as the working fluid, taking into account the main losses in the engine chamber with a pressure of up to 1 MPa and a high gas-dynamic pressure drop ratio of  $\delta = 10^4$ .

The energy characteristics of such a light receiver-battery are improved in comparison with a single-stage one due to lower losses to reverse thermal radiation, increasing its efficiency with lower mirror accuracy, and simplifying the conditions for tracking the Sun [11].

Fig. 1 shows the STRE diagram with two stages of heating of the CATS system. Hydrogen is initially heated to the melting point of lithium hydride (961 K) in the peripheral region, and then, in the second stage of the TES, it is further heated to the final melting point of beryllium oxide (2804 K). Heated hydrogen, when expanding in the nozzle, creates thrust P, which, in combination with the thermal discharge time of the accumulator  $t_{\text{prop}}$ , provides a single thrust impulse  $I_{\text{single}} = P \cdot t_{\text{prop}}$  at each active section, depending on the specified time of the interorbital flight.

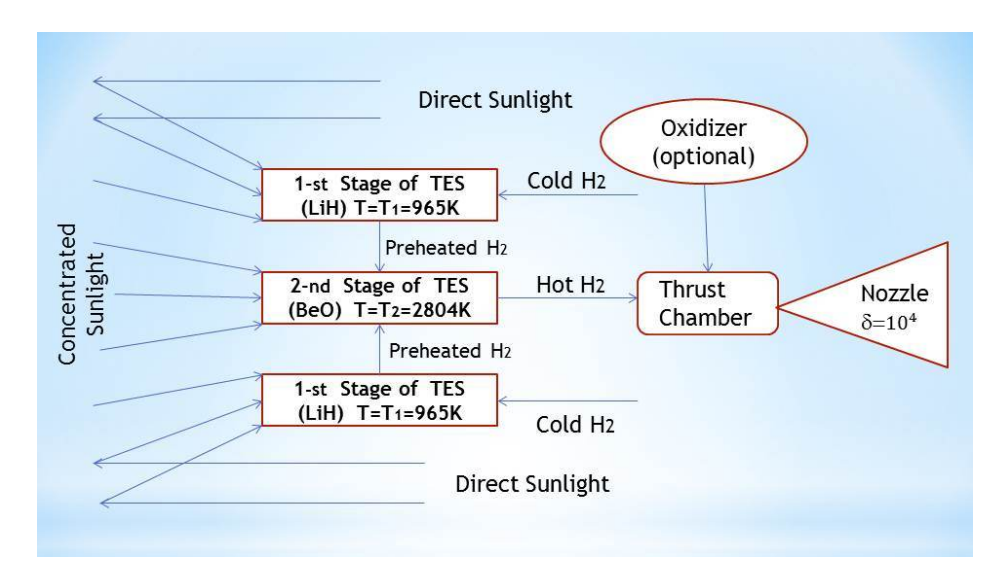


Рис. 1. СТРД с двумя ступенями нагрева теплового аккумулятора

Fig. 1. STRE with double-staged TES

### Selecting parameters of CATS system and heat-accumulating materials

Table 1 shows the temperature values that are most suitable for the TES first stage while the second stage temperature is 2804 K, depending on its relative radius R and the accuracy parameter of the concentrator  $\Delta\alpha$  (according to O. I. Kudrin, based on a generalized mathematical model of the concentration process shared with A. V. Nikiforov and E. V. Tveryanovich [5; 12]) at the adopted value of the semi-opening angle of the paraboloid aperture  $\Theta = 60^{\circ}$ .

The value of the angle  $\Theta = 60^{\circ}$  was chosen as rational, since long-focus mirrors ( $\Theta = 45^{\circ}$ ) require greater longitudinal and transverse accuracy of orientation to the Sun and are characterized by a large focal length  $F_I$ , and short-focus mirrors ( $\Theta = 70^{\circ}$ ) increase the absorbing area of the light receiver-accumulator with the corresponding thermal losses due to reverse intrinsic radiation. In this case, for short-focus mirrors with large angles  $\theta_{\text{max}} > 60^{\circ}$ , the shift in the maximum density of the luminous flux in focus during misorientation of the CR system will be smaller, and larger mirror opening angles correspond to smaller "critical" values of the accuracy parameter, above which it is advisable to use a light receiver with non-uniform heating of the surface. However, the average concentration of solar energy  $C_{\text{av}}$  at large  $\Theta > 60^{\circ}$  decreases significantly, and the total area and mass of the mirror increase. The average concentration level must be sufficient to melt the high-temperature second-stage HAM.

The radius of the first (low-temperature) stage is determined from the energy balance for the stages, taking into account the maximum radius of the focal light spot  $R_{\text{max}}$  with 2- $\sigma$  standard Gaussian deviation of the concentrated light beams from the focus of the paraboloid (up to 95.4% of the incident solar energy is captured by the light receiver). As Table 1 demonstrates for a given melting temperature of low-temperature HAM, the relative radius of the high-temperature stage  $R = R_1/R_{\text{max}}$  decreases with an increase in the parameter  $\Delta\alpha$ , where  $R_1$  is the radius of the second (high-temperature) stage of the light receiver-accumulator. The radius Rmax, taken as a first approximation to be equal to the radius of the input aperture of the light receiver (the outer radius of the annular low-temperature stage), increases with an increase in the parameter  $\Delta\alpha$  due to the decompression of the radiant light flux diagram. It should be noted that an increase in the angle  $\Theta$  also leads to an increase in  $R_{\text{max}}$ , which will require complex optimization according to a particular criterion – the minimum mass and dimensional parameters of CATS system at the stage of preliminary design. The  $R_{\text{max}}$  values presented in Table 2 depend on the paraboloid diameter, hypothetically taken to be 12 meters, which is quite typical for the task of transferring to a geostationary orbit. In this case, it is necessary to consider the focal length of

the mirror  $F_1$ , which affects the accuracy of tracking the Sun, and the level of average concentration of solar radiation C<sub>av</sub>, which shows the possibility of heating the gas to the required temperature.

Optimum temperature of the 1st stage of TES, K

Table 1

Table 2

	R = 0.1	R = 0.15	R = 0.2	R = 0.25	R = 0.3	R = 0.33	R = 0.35	R = 0.4	R = 0.45
$\Delta \alpha = 0.5^{\circ}$	2018	2000	1981	1937	1880	1810	1760	1701	1542
$\Delta \alpha = 0.6^{\circ}$	1921	1904	1881	1835	1772	1685	1594	1560	1324
$\Delta \alpha = 0.7^{\circ}$	1858	1835	1795	1737	1668	1558	1472	1407	970
$\Delta \alpha = 0.8^{\circ}$	1767	1762	1713	1664	1571	1444	1332	1190	960
$\Delta \alpha = 0.9^{\circ}$	1709	1690	1647	1585	1494	1345	1144	967	400
$\Delta \alpha = 1.0^{\circ}$	1608	1560	1474	1353	1094	961	_	_	_
$\Delta \alpha = 1.1^{\circ}$	1561	1522	1449	1307	1063	_	_	-	_
$\Delta \alpha = 1.2^{\circ}$	1510	1457	1375	1199	965	_	_	_	_

Optical parameters of the CR system

	•		
),8°	$\Delta \alpha = 0.9^{\circ}$	$\Delta \alpha = 1.0^{\circ}$	$\Delta \alpha = 1,1^{\circ}$
9	0.150	0.160	0.171
4	7.24	7.24	7.24
9	1599	1392	1231

	$\Delta \alpha = 0.6^{\circ}$	$\Delta \alpha = 0.7^{\circ}$	$\Delta \alpha = 0.8^{\circ}$	$\Delta \alpha = 0.9^{\circ}$	$\Delta \alpha = 1.0^{\circ}$	$\Delta \alpha = 1,1^{\circ}$
$\Theta = 45^{\circ}$	0.118	0.129	0.139	0.150	0.160	0.171
$R_{\rm max}$ , M	7.24	7.24	7.24	7.24	7.24	7.24
$F_1$ , м $C_{\rm av}$ [-]	2557	2160	1879	1599	1392	1231
$\Theta = 60^{\circ}$	0.137	0.149	0.161	0.170	0.190	0.20
$R_{\rm max}$ , M	5.20	5.20	5.20	5.20	5.20	5.20
$F_1$ , м $C_{\rm av}$ [-]	1918	1620	1386	1199	1048	923
$\Theta = 70^{\circ}$	0.185	0.200	0.217	0.23	0.25	0.266
$R_{\rm max}$ , M	4.28	4.28	4.28	4.28	4.28	4.28
$F_1$ , м $C_{\rm av}$ [-]	1023	864	739	640	559	459

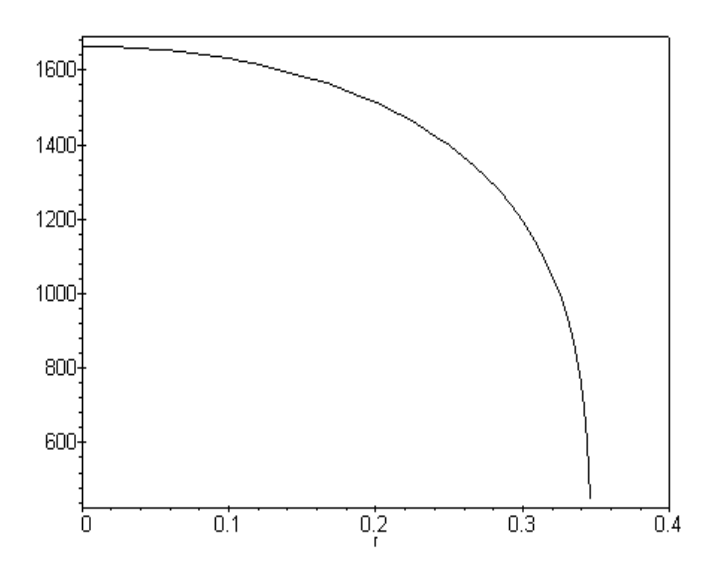


Рис. 2. Зависимость оптимальной температуры первой ступени от относительного радиуса Rпри значениях параметра  $\Delta \alpha = 1^{\circ}$  и угла  $\Theta = 60^{\circ}$  для температуры плавления BeO

Fig. 2. Dependence of TES first stage optimal temperature on relative radius R at accuracy parameter  $\Delta\alpha=1^o$  and angle  $\Theta=60^o$  for  $\mbox{\it BeO}$  melting temperature

The problem of choosing the accuracy parameter of the concentrator  $\Delta\alpha$  is a compromise between the conflicting requirements for the size of the concentrator and its specific and total mass, since a decrease in the parameter  $\Delta\alpha$  leads to an increase in the efficiency of the light receiver and, as a consequence, a decrease in the area of the mirror, but, at the same time, to a nonlinear increase in its specific mass. On the other hand, an increase in  $\Delta\alpha$  leads to a decrease in the actual temperature of the hydrogen at the outlet, which determines the specific impulse of the engine and the mass flow rate of the heated gas, and to ensure constant thrust it is necessary to increase the size of the mirror, and a decrease in its specific mass, on the contrary, should reduce the total mass of the CR system. Therefore, it is advisable to use the "concessions" method here – to determine to what extent it is required to increase the energy efficiency of the engine given design, technological, operational and other limitations. We should also take into consideration the relationship between the accuracy of the mirror and the requirements for precision tracking of the solar system by the CATS.

For a two-stage light receiver in the range  $\Delta \alpha = 0.8-1.1^{\circ}$ , the energy-mass efficiency of the spacecraft with the considered STP changes insignificantly. The mass of the fueled solar propulsion system (SPS) with a two-stage light receiver has a minimum in the specified range of  $\Delta\alpha$  values. The minimum mass of the engine with the concentrator corresponds to the values  $\Delta \alpha = 1.3-1.4^{\circ}$ , however, against the background of large masses of the SPS, this factor is not of decisive importance. Therefore, according to the condition of maximum mass of the payload, it is possible to select  $\Delta \alpha = 1^{\circ}$  as the calculated value, taking into account the technological requirements for the accuracy of the mirror as well. Then the average concentration of solar radiation at  $\Theta = 60^{\circ}$  is equal to  $C_{SR} = 1$ : 1048, which corresponds to a surface energy density of 1.425 MJ/m<sup>2</sup>, sufficient to heat the central stage to the melting temperature of beryllium oxide. The technological feasibility of providing a high level of concentration using inflatable thin-film structures has been experimentally confirmed underground conditions at the experimental cryogenic-vacuum stand "TA-1 Tank-6" and the optical-mechanical stand FSC of SRS Technologies, as a subcontractor of the Thiokol Propulsion corporation, with funding from AFRL/PRSS and NASA Glenn Research Center within the framework of the NASA Shooting Star, SOTV, STUS and other programs (USA), for testing the power source of the STP – the "mirror concentrator-light receiver" system. The concentration level of the inflatable thin-film mirror in these studies was about 3000 "suns" [13-15].

For practical application of the STP, it should be also taken into account the decrease in the accuracy of the film concentrator during long-term operation in space conditions, which has a greater impact on precision mirrors (with a smaller parameter  $\Delta\alpha$ ), therefore the choice of  $\Delta\alpha=1^{\circ}$  seems appropriate, including the operating conditions. Based on the Table 1 data, for this case the relative radius of the high-temperature stage is R=0.33.

In general, a mirror concentrator is a paraboloid truncated by a cone or cylinder [16]. In order to ensure its stable operation in the deployed state with hydrogen pressurization, the outer surface of the working segment is covered with a thin layer of epoxy resin-based polymer that hardens in space conditions under the influence of harsh ultraviolet radiation [5]. We could note that for technological simplification, the concentrator can in some cases be designed as a pseudo-spherical structure; this requires the corresponding development of a stepped axial-type light receiver-accumulator, which requires specialized research.

In the case under consideration, an off-axis bi-concentrator STP design with two reflecting surfaces located symmetrically relative to the longitudinal axis of the spacecraft is appropriate [2]. In this case, it is possible, in particular, to significantly reduce the size of two independent CATS systems with two nozzle blocks for a given software control of the thrust vector along the trajectory.

Table 3 presents the thermophysical properties of heat-accumulating materials that are most suitable for use in STP. Comparing the data in Tables 1–3, it follows that it is advisable to use lithium hydride in the first (low-temperature) heating stage of the TES and beryllium oxide for the second stage due to the highest values of the latent heat of melting and the technological possibility of placing different-temperature HAMs in a two-stage battery, taking into account that for TES with LiH and BeO the relative radius is quite large (R = 0.33). The total radius of the central high-temperature stage is determined with a known value of the maximum size of the focal light spot  $R_{max}$ , which depends on the geometric parameters of the solar concentrator.

Table 3

**HAM features for STP** 

HAM	Melting point, K	Heat of melting, kJ/kg
Lithium hydride LiH	961	2540
Lithium fluoride LiF	1118	1030
Beryllium Be	1555	1512
Silicon Si	1700	1782
Titanium silicide TiSi <sub>2</sub>	1818	1116
$Al_2O_3$ -4 $BeO$ -4 $MgO$	1918	1440
$Al_2O_3$ -4 $BeO$ - $MgO$	2033	1530
3BeO-2MgO	2153	2088
Eutectic B-Si	2320	2540
Beryllium oxide BeO	2804	2840
Magnesium oxide MgO	3070	1922

The paper [7] presents a generalized object-oriented mathematical model for determining the energy-ballistic efficiency of a spacecraft with a solar propulsion system at the top level of the hierarchy, intended for carrying out mass variant calculations when choosing the appropriate design of a spacecraft with a solar propulsion system. When analyzing processes in the TES with refined calculations at lower levels of the mathematical model, it is necessary to solve the Stefan problem with a moving zone of separation of the liquid and solid phases during the process of "charging-discharging" the battery. In particular, a non-stationary two-dimensional thermal-hydrodynamic model of the melting-crystallization processes HAM was developed at the State Research Institute of Luch Scientific Production Association [4; 17]. In case of evaluation variant calculations, a simplified one-dimensional mathematical model [5] is sufficient, which allows to determine the dimensions of the TES and evaluate its main thermophysical processes, considering, for example, a capsule or shell-and-tube arrangement of heat-accumulating materials.

It may be possible to use materials for the peripheral stage that are higher in temperature than LiH, such as Si, Be and some others, in combination with a central heating stage based on beryllium oxide or compositions such as B\*Si, 3BeO-2MgO, Al2O3-4BeO-MgO. Due to Table 1, the required accuracy parameter  $\Delta\alpha$  and the relative radius R change, and the TES mass increases in accordance with the lower latent heat of melting, which affects the final mass of the payload. In addition, with an increase in the temperature of the first stage, the degree of non-uniform temperature of the CATS system decreases, which negatively affects the efficiency of the system. The specific impulse of the engine's thrust is determined by the choice of the HAM of the central stage.

When selecting HAMs, the stability of their physical and chemical properties under temperature changes and phase transitions should be considered, as well as their thermomechanical and corrosion compatibility with the battery's structural materials.

#### Spacecraft features with STP with a two-stage CATS system

We research the use of the medium-class launch vehicle Soyuz-2.1b to be launched from the Bai-konur Cosmodrome. The mass of the spacecraft – the upper stage with the SPS and the payload (PL) – in low reference orbit (LEO) is 8000 kg. The target is the geostationary orbit (GEO). The maximum payload mass was adopted as the criterion for the effectiveness of the LEO-GEO mission. The flight time  $T_{\Sigma}$ , accepted as an unconditional limitation, varies from 20 to 90 days. The illumination conditions of the transfer orbits are determined by the launch time of the launch vehicle, taking into account partial shading by the Earth, and depend on the osculating elements of the transfer orbits. Fig. 3 shows the dependence of the payload mass launched into geostationary orbit using a "solar" booster unit – a spacecraft – on the ratio of the mass of the solar concentrator  $M_k$  to the mass of the heat accumulator  $M_a$  (we will express it by the parameter  $[p] = M_k/M_a$ ) and the value of the unit thrust impulse  $I_{single} = P \cdot t_{prop}$  in each active section. The value of the engine switching time during thermal discharge

of the battery  $t_{prop}$  depends on the total energy capacity of the TES, determining its mass and, through the parameter [p], the mass of the concentrator  $M_k$ . The thrust P depends, among other things, on the heating temperature of the hydrogen in the high-temperature stage of the battery. The selection of appropriate values for the specified parameters is carried out using regular optimization methods.

In general, a complex variation of the values of  $I_{single}$  and the parameter [p] is required, since the same flight time and PL mass may correspond to different combinations of  $\{I_{single},[p]\}$ . As Fig. 3 shows, a smaller unit impulse of the engine corresponds to a larger mass of the payload in the destination orbit for any values of the parameter [p]. However, it is necessary to take into account the flight time T and the dimensions of the CATS system. For practical purposes, it is significant to select acceptable dimensions of the solar concentrator, on which the inertial properties of the spacecraft and the ability to precisely track the solar disk during the charging of the TES depend. It is also necessary to take into account the fundamental possibility of creating a TES with acceptable mass-dimensional and thermal-physical characteristics. Therefore, in addition to maximizing the mass of the payload, as in the case of selecting the parameter  $\Delta\alpha$ , we propose to use the "concessions" method – to evaluate the level of possible acceptable reduction in the efficiency of the flight task with a certain simplification of the control and automation system, as the most complex element of the engine.

For identical combinations  $\{I_{single}, [p]\}$  the main features of the spacecraft with STP remain unchanged, namely:

- flight time  $T_{\Sigma}$ ;
- PL mass  $M_{\rm pl}$ ;
- concentrator diameter  $D_c$ , its focal parameter  $F_1$  and mass  $M_k$ ;
- total energy capacity of the TES  $Q_a$  and its mass  $M_a$ ;
- distribution of energy across heating stages  $Q_{a1}$  and  $Q_{a2}$ ;
- power of the light receiver-battery  $N_{\text{receiver}}$ ;
- effective specific impulse  $I_{\text{specific(eff)}}$ ;
- number of orbital turns for TES charge;
- number of STP ignitions in the apsidal regions;
- total time of TES charging considering the shading of transfer orbits.

Therefore, the aim of further research is to determine rational combinations  $\{I_{single},[p]\}$  corresponding to the tactical-technical and technical-economic assignment, taking into account technological and other conditions, allowing the creation of a spacecraft with the studied propulsion to perform energy-consuming flight tasks such as a flight to GEO.

The mass mathematical model of the spacecraft (the upper stage with the SPS and the payload placed on it) is accepted as statistical and is based on the research [18; 19]. The upper stage contains a fuel tank with a working fluid (liquid hydrogen), a STP and CATS system, elements of a pneumatic hydraulic system with receivers, dampers and pump-compressor equipment with drives, a control system, a system for ensuring the spacecraft's thermal regime, on-board cable networks, structural elements, and other elements (parts of the automation system, thermal insulation, general assembly parts). A more detailed mass summary is compiled when selecting a specific spacecraft scheme. For a sufficiently long flight of 60–90 days, an adjustment is also necessary for the evaporation of some of the cryogenic hydrogen. The mass model of the spacecraft is based on the given equations, reflecting the linearized connections according to the main parameters. The accuracy of a mathematical model depends on the accuracy of statistical coefficients that bring strict analytical relationships into line with statistical data.

Fig. 4 shows the 3D-dependence of the payload mass on the temperature of the central stage and the parameter  $\Delta\alpha$  for the case of  $T_{\Sigma}=60$  days, this results in the possibility of a certain change in these values in a fairly narrow range with an insignificant change in the useful mass output to the GEO, which makes it possible to vary, for example, the accuracy parameter, at subsequent stages of engine design.

The values of the mirror diameter  $D_{c1}$  for the off-axis biconcentrator scheme [2] are presented in Fig. 5 as functions of a number of combinations  $\{I_{single}, [p]\}$ . When choosing these values, it is neces-

sary to evaluate the technological feasibility of creating and deploying large-scale film structures in space. A larger concentrator diameter corresponds to a longer focal length  $F_1$ , which directly affects tracking the position of the solar disk during orbital movement. As noted above, the maximum size of the focal spot  $R_{\text{max}}$ , which affects the ratio of the sizes of the TES stages, depends on the values of  $D_{\text{cl}}$  and  $F_1$ .

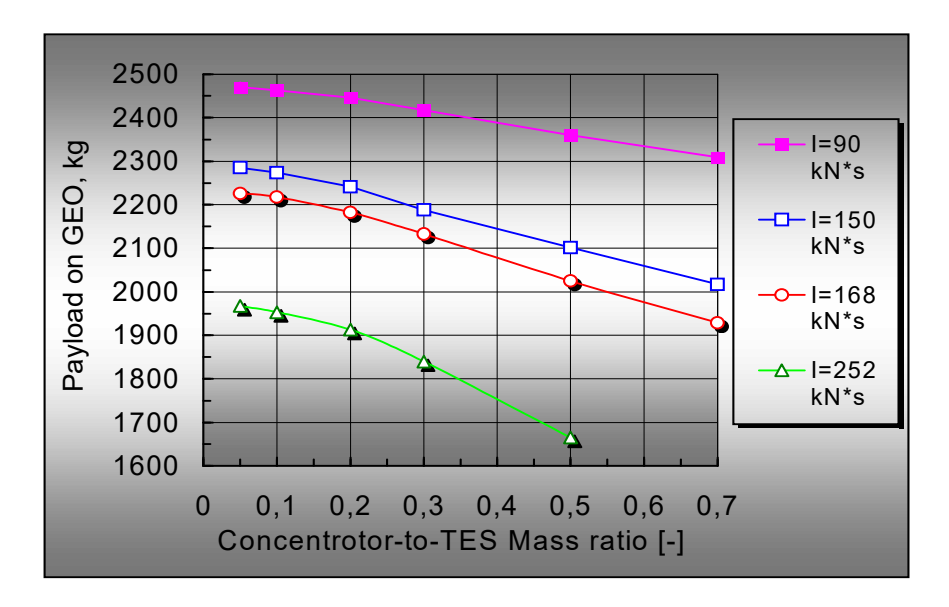


Рис. 3. Зависимость массы КА на  $\Gamma$ CO от отношения массы концентратора к массе двухступенчатого теплового аккумулятора с ТАМ на основе LiH+BeO

Fig. 3. Payload mass on GEO vs. concentrator-to-TES mass ratio for HAM based on *LiH* and *BeO* 

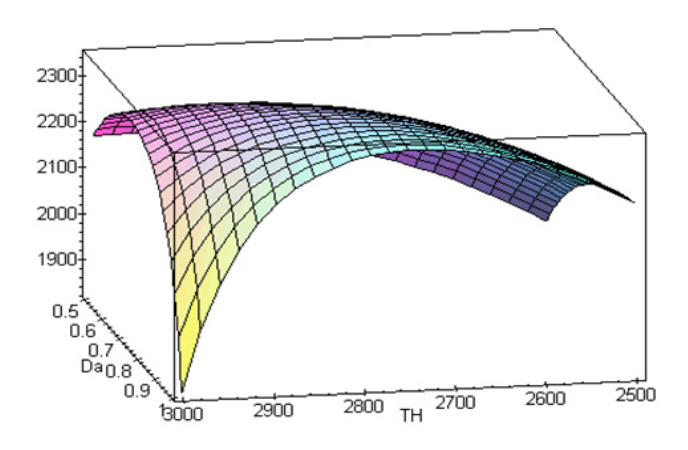


Рис. 4. Масса ПН как функция параметра точности СТРД с двухступенчатой системой КПА и температуры нагрева водорода для времени перелета 60 суток

Fig. 4. Payload mass on GEO as a function of STP accuracy parameter and hydrogen heating temperature for 60 days trip time

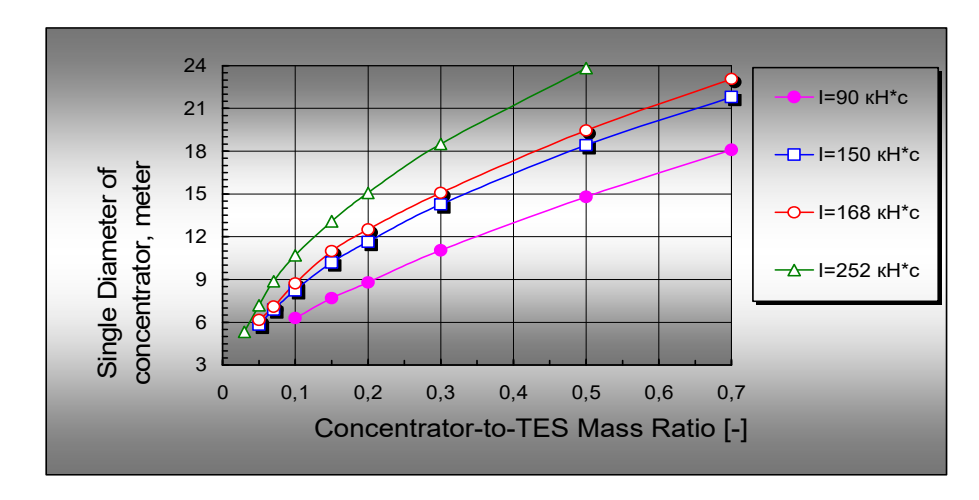


Рис. 5. Зависимость диаметра солнечного концентратора  $D_{\kappa l}$  от параметра [p]

Fig. 5. Dependence of concentrator diameter  $D_{c1}$  on parameter [p]

The time of payload withdrawal to the GEO  $T_{\Sigma}$  depends significantly on the combination  $\{I_{single},[p]\}$ . Fig. 6 demonstrates the rational range of values of the parameter [p], which is 0.1–0.3. An increase in the parameter [p] does not lead to a noticeable reduction in the time it takes to launch the payload into geostationary orbit, while a decrease in [p] < 0.1 is accompanied by a significant increase in the flight time, which makes the STP insufficiently competitive with regard to the electric propulsion systems (EPS) and chemical engines with the "additional launch" of the payload into high orbits using onboard EPS.

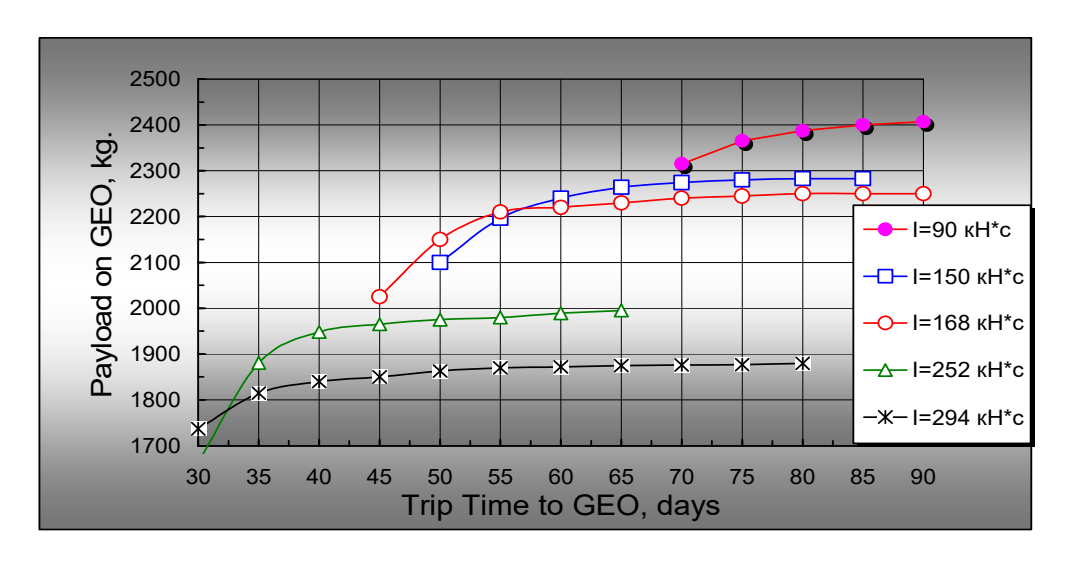


Рис. 6. Зависимость времени перелета на  $\Gamma$ CO от параметра [p]

Fig. 6. Dependence of LEO-to-GEO trip time on parameter [p]

The payload mass depends on the flight time according to the dependencies shown in Fig. 7, for different values of the single thrust impulse with a corresponding change in the parameter [p]. The results in Fig. 3, 5 and 6 demonstrate that varying the combination  $\{I_{single}, [p]\}$  allows to identify areas of appropriate values of thrust and discharge time of the TES in the field of values  $\{M_{pl}, D_c\}$ . Small values of  $I_{single} < 90$  kN\*s are only advisable for flight time exceeding 90 days, which requires solving complex technical problems of storing cryogenic hydrogen. Large values of  $I_{single} > 300$  kN\*s are typi-

cal for the case of  $T_{\Sigma}$ < 30 days with a significant reduction in the mass of the payload. Thus, for  $T_{\Sigma}$ = 20 days we have rational values  $I_{single}$  = 390 kN\*s at [p] = 0.3, corresponding to a PL mass of 1250 kg.

Due to the analysis of the presented results it follows, in particular, that for a flight time of  $T_{\Sigma} = 30$  days, the values  $I_{single} = 240$ –270 kN\*s and the values of the parameter [p] in the vicinity of [p] = 0.25 are appropriate to launch a payload with a mass of about 1720 kg. The shorter flight time is associated with a sharp decrease in the energy-mass efficiency of the spacecraft.

For the time  $T_{\Sigma} = 60$  days, it is advisable to select the values  $I_{single} = 140-160$  kN and the parameter [p] in the vicinity of [p] = 0.2, which ensures the mass of the PL of about 2180 kg. An increase in flight time is followed by an asymptotic increase in the mass of the payload being launched. Smaller values of the single thrust impulse of the engine  $I_{single} = 90$  kN and the parameter [p] = 0.12 correspond to a longer flight time (up to 90 days) with a useful mass  $M_{\rm PL} = 2300-2320$  kg.

Therefore, for the flight time of  $T_{\Sigma} = 20$ –90 days, the ranges of values within  $I_{single} = 90$ –400 kN\*s and [p] = 0.1–0.3 are appropriate.

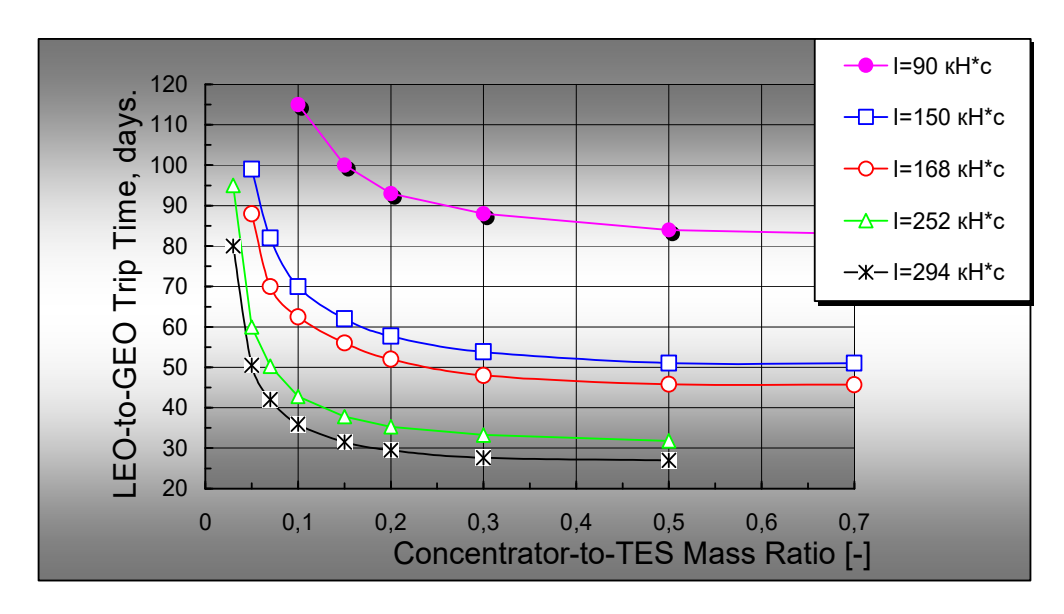


Рис. 7. Зависимость массы ПН от времени перелета на ГСО

Fig. 7. Payload mass on GEO vs. LEO-to-GEO trip time

The mass of the heat accumulator  $M_a$  is the main component of the total mass of the heat accumulator and is determined by its total energy capacity  $Q_a$  and the specific latent heat of fusion of the used HAM. In addition, it is necessary to take into account the mass of the structure and high-temperature thermal insulation, consisting, for example, of pyrographite in combination with graphite and zirconium dioxide felt [3]. In this case, the total mass of the TES can increase to 50–70% of the mass of the HAM in both heating stages. Optimization of the design and thermal insulation is performed at lower levels of the mathematical model according to specific criteria that are subordinate to the criterion of a higher level – the minimum mass of the TES and the design of the "solar" upper stage.

Fig. 8 shows the dependencies of the total TES mass on the appropriate values of the thermal discharge time and the thrust level of the STP, showing the values of a single thrust impulse and its relationship with other quantities in accordance with Fig. 3, 5–7. In the considered interval of engine operation time, with each thermal discharge of the TES, it is possible to use in calculations the impulse approximation of active maneuvers with correction for gravitational losses of speed at the pericenter of transfer orbits [19; 20].

Table 4 presents the selected parameters of the spacecraft with a STP for a flight time of 20 to 90 days. With an increase in  $T_{\Sigma}$  within the limits under consideration, these parameters change significantly. The single thrust impulse  $I_{\text{single}}$  is reduced due to the reduction of thrust and the thermal dis-

charge time of the TES. The PL mass increases significantly. Increasing the time  $T_{\Sigma}$  from 20 to 90 days, we can observe an increase in the relative values of  $Q_a/N_r$ ,  $Q_a/M_k$ ,  $Q_a/F_k$  (here the designations  $N_{\rm p}$ ,  $M_{\rm k}$ ,  $F_{\rm k}$  are used as the thermal power of the CATS system, the mass of the concentrator and the area of its aperture), characterizing the integral indicators of the engine, by 2.4 times, which is caused by a more significant decrease in the size and mass of the concentrator compared to the rate of decrease in the energy capacity of the TES. For any flight time, the ratio of the energy capacity of the second (high-temperature) stage  $Q_{a2}$  exceeds the energy capacity of the first stage  $Q_{a1}$  by 2.33 times, and for a given unit thrust impulse  $I_{\text{single}}$  does not depend on the parameter [p], as does the total energy capacity of the battery  $Q_a$  and its mass  $M_a$ . The thermal power of the CATS system decreases with increasing time  $T_{\Sigma}$  in accordance with the decrease in the required area of the reflective surface of the solar concentrator in the specified range of time  $T_{\Sigma}$ . The specific mass of the concentrator by power, as the ratio of its total mass (at an optimal ratio with the mass of the TA) to the thermal power of the receiver, is about 1 kg/kW. The focal length  $F_1$  indicated in Table 4, which decreases due to the decrease in  $D_{c1}$ , is an important parameter since, as noted above, it significantly affects the accuracy of the orientation of the CATS system to the Sun, which is important under conditions of thermal stress in the trusses supporting the power torus of the solar concentrator, and can become one of the limitations for the flight time.

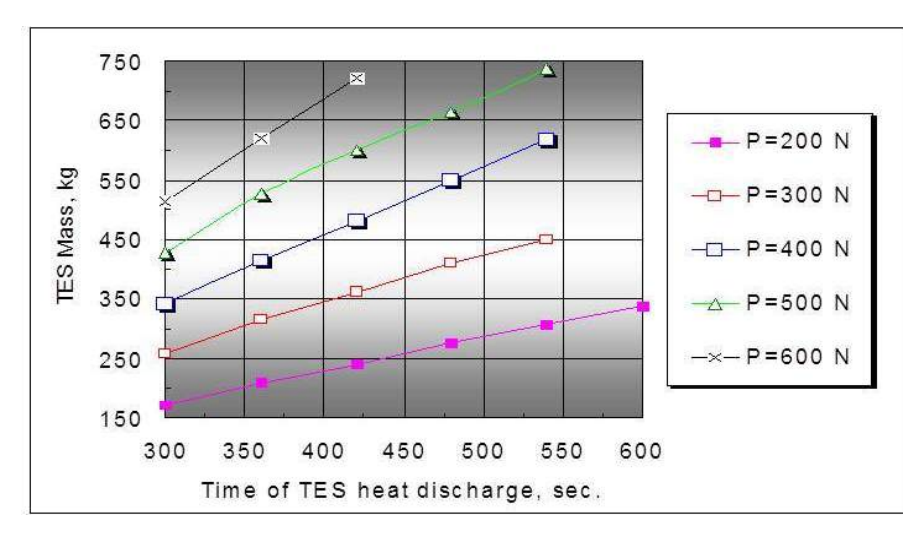


Рис. 8. Зависимость массы ТА от тяги и времени работы СТРД

Fig. 8. Dependence of the TES mass on the STP thrust and burn time

Tables 4 and 1 make it possible to determine the radius of the low-temperature stage, provided that it is consistent with the size of the focal spot  $R_{\text{max}}$ , as well as the radius of the central stage  $R_1$ . The radius  $R_1$  is determined from Table 1 based on the values of the relative radius R for the accepted value of the parameter  $\Delta \alpha = 1^{\circ}$  and the melting temperature of lithium hydride. Based on these values, the remaining geometric and thermophysical characteristics of the TES are determined, which are necessary for calculating its working process at a level of accuracy sufficient for carrying out mass variant calculations.

The values of the effective specific impulse  $I_{\text{specific (eff)}}$ , as the ratio of the total thrust impulse to the mass of the fueled solar propulsion system (SPS), show the integral mass-energy efficiency of the spacecraft, which is significantly higher compared to a liquid propellant rocket engine (about 3000 m/s), but worse than the indicators of a spacecraft with an electric propulsion system (EPS) of the size of the СПД-140Д (over 7000 m/s) [21]. Moreover, the flight time of a spacecraft with a STP to a geostationary orbit is significantly shorter compared to the use of electric rocket propulsion (up to 180 days) or their combination with chemical propulsion. Therefore, during the final launch into GEO, a

spacecraft with a combined system including high-thrust and low-thrust engines, with a time of  $T_{\Sigma}$  = 60 days and identical launch conditions, can launch 1,640 kg of payload [22], while a STRD with a two-stage CATS system is capable of delivering a payload weighing up to 2180 kg with the same flight time. At time  $T_{\Sigma}$  = 90 days, the values of the PL mass are 1870 kg and 2320 kg, respectively. For comparison, it can be noted that when using the Soyuz-2.1b launch vehicle with the Fregat-M upper stage, the payload mass in geostationary orbit is 1060 kg.

Reasonable parameters of a spacecraft with STP

Table 4

Flight time,	$t_{\mathrm{prop}},$	Thrust,	Thrust	Parameter	$N_{\rm r}$ ,	$Q_{\mathrm{a}},$	$Q_{\rm al}/Q_{\rm a2},$	TES
days	sec	N	impulse,	[ <i>p</i> ]	kW	MJ	MJ/MJ	mass, kg
			kN·sec	$(M_{\scriptscriptstyle  m K}/M_{ m a})$				
20	650	600	390	0.30	325	1977	593/1384	1080
30	540	500	270	0.25	187	1368	410/958	749
45	500	380	190	0.22	116	963	289/674	526
60	480	300	144	0.20	80	730	219/511	392
90	420	260	109	0.12	38	554	166/388	297

## Table 4 (continuation)

#### Reasonable parameters of a spacecraft with STP

Flight time, days	$Q_{\rm a}/N_{\rm r},$	$Q_{\rm a}/M_{\scriptscriptstyle  m K},$	$Q_{\rm a}/F_{\rm \kappa}, \ { m MJ/m}^2$	$Q_{\rm a}/M_{\rm a},$	$I_{\text{specific(eff)}}$ , m/s
	MJ/kW	MJ/kg	$MJ/m^2$	MJ/kg	
20	6.08	6.095	2.438	1.828	5326
30	7.30	7.314	2.925	1.828	5772
45	8.29	8.311	3.324	1.828	6090
60	9.12	9.142	3.657	1.828	6286
90	14.60	14.628	5.851	1.828	6573

Table 4 (continuation)

#### Reasonable parameters of a spacecraft with STP

Flight time, days	$R_{\rm max}$ , m	$R_1$ , m	$F_{\kappa 1}$ , m	$D_{\kappa 1}$ , m	PL mass, kg
20	0.350	0.116	9.83	22.70	1250
30	0.267	0.088	7.47	17.25	1720
45	0.209	0.069	5.88	13.60	2015
60	0.174	0.058	4.88	11.27	2180
90	0.120	0.040	3.36	7.76	2320

Table 4 shows the possibility of delivering a wide range of spacecraft to geostationary orbit using the Soyuz-2.1b medium-class launch vehicle with a solar booster unit instead of using heavy and expensive launch vehicles with chemical boosters (CB). Thus, within 20 days of flight, it is possible to deliver a payload to geostationary orbit weighing up to 1.250 kg (for example, a relay satellite of the Luch-5 series weighing 1,150 kg developed by JSC Reshetnev), launched by a heavy Proton-M launch vehicle with a Briz-M upper stage. 30 days is enough to launch a spacecraft weighing approximately 1.700 kg (for example, a hydrometeorological satellite of the Electro-L type, delivered by a 3ehut-3SLbΦ launch vehicle with a Fregat-SB upper stage, or a Proton-M launch vehicle with a ДМ-03 upper stage). Spacecraft of the Express-AMY-7 type, weighing 1.976 kg, can be delivered to GEO within 45 days of flight. The launch of the Express-AMY-3 communications and television broadcasting satellite weighing 2,154 kg (maximum weight up to 2.250 kg), delivered by the Proton-M launch vehicle with the Briz-M upper stage, is possible within 60 days. A payload mass of 2.340 kg is typical for a geostationary satellite of the Raduga-1 type, launched by a Proton series launch vehicle with a ДМ

upper stage based on the KAYP-4 platform. Launching such a vehicle using a STP would require 90 days. Heavy satellites of the Express-AM series, weighing 2,579 kg, could be launched into geostationary orbit in a longer time using the Soyuz-2.1b launch vehicle together with sustain EPS and STP, such as the ИД-500 ion engine (developed by the Keldysh Research Center), with a deep "final" boost to the target orbit.

#### Comparative characteristics of alternative STP schemes

We could compare the efficiency of using different types of SPS under the same conditions: a specific impulse of 900 s and a flight time to GEO of  $T_{\Sigma}=60$  days. The heating time of the TES and the number of orbital turns required for the complete melting of the HAM are determined by the ratio  $Q_a/N_r$ , and for an engine with a two-stage accumulator it is equal to  $Q_a/N_r=9.12$  MJ/kW. In the case of a single-stage beryllium oxide-based STP, the  $Q_a/N_r$  ratio is about 23 MJ/kW. The efficiency of the CR of such a propulsion is  $\eta_{\text{receiver}}=0.264$  (for a two-stage CATS system  $\eta_{\text{receiver}}=0.326$ ). Also indicative are the  $Q_a/F_k$  ratios, which show the amount of radiant energy from the concentrator necessary to provide the required single pulse  $I_{\text{single}}$ , amounting to 3.65 and 7.50 MJ/m<sup>2</sup>, respectively. The ratios  $Q_a/N_r$  and  $Q_a/F_k$  are determined mainly by the type of phase-change materials and the accuracy of the mirror.

For a single-stage STP with a beryllium oxide TES with an optimal accuracy parameter  $\Delta\alpha=0.25^\circ$ , the rational values are [p]=0.8 and  $I_{\text{single}}=192 \text{ kN} \cdot \text{s}$ . The payload mass in the case of using a single-stage STP with BeO for a flight to GEO is 1950 kg with a mirror diameter of about 9 meters. It should be noted that with the optimal mirror accuracy parameter  $\Delta\alpha=0.25^\circ$ , the permissible misorientation of the CATS system from the aiming direction to the Sun in the dynamic tracking mode does not exceed  $\beta<0.8^\circ$  (in the static tracking mode  $\beta_{\text{static}}=0.2^\circ$ ). In the case of a propulsion with a two-stage CATS system, the rational value of the parameter  $\Delta\alpha=1^\circ$  allows for a misorientation within the limits of  $\beta=\pm1.64^\circ$  (in the static tracking mode  $\beta_{\text{static}}=\pm0.41^\circ$ ) without taking into account the longitudinal and transverse defocusing of the light receiver in relation to the mirror, and it is quite feasible with modern technical means [9]. For rough dynamic orientation, a 6-degree-of-freedom «hexapod» can be used [23], while fine orientation is provided by a light receiver with «auto-tracking» properties, using, in particular, bimetallic drives [12].

We note, in particular, that for a sufficiently effective STP with a single-stage TES based on the B\*Si eutectic (optimal mirror accuracy  $\Delta\alpha=0.5^{\circ}$ , parameter [p]=0.3 and  $I_{\text{single}}=168 \text{ kN}\cdot\text{s}$ ) with a melting temperature of 2320 K and a specific energy capacity of 2540 kJ/kg, the PL mass can reach 2010 kg with a diameter  $D_{k1}=9$  m. In this case, the ratio  $Q_a/F_k=12.15 \text{ MJ/m}^2$ , and the ratio  $Q_a/N_r=7.8 \text{ MJ/kW}$ . The permissible angular misalignment of the CATS system when tracking the Sun can reach  $\beta=1.1^{\circ}$  (in static tracking mode  $\beta_{\text{static}}=0.27^{\circ}$ ).

If STP obtains the simplest equal-temperature receiver without TES, the mass of the PL is 1600 kg with an optimal temperature of the light receiver of 2200 K and a parameter  $\Delta\alpha = 0.64^{\circ}$ . The concentrator diameter is 14.8 meters. The accuracy of tracking the Sun in dynamic tracking mode should be no worse than  $\beta = \pm (1-1,25)^{\circ}$ .

A spacecraft with a two-stage STP without TES, with the previously adopted values of the parameter  $\Delta\alpha=1^{\circ}$ , the hydrogen heating temperature of 2800 K and the angle  $\Theta=60^{\circ}$ , which determine the efficiency of the "concentrator-light receiver" system  $\eta=0.326$ , ensures the launch into geostationary orbit of a payload weighing approximately 2100...2150 kg with a mirror diameter of approximately 15 meters. The accuracy of the permissible orientation to the Sun, as in the case of the two-stage CATS system, is  $\beta=1.64^{\circ}$ .

To compare the parameters of solar thermal propulsion of different designs, it is necessary to note the technical capabilities of the STP with an extremely unequal-temperature multi-stage "concentrator-receiver" system without a TES, which has the best characteristics that completely take into account the energy level and the focal irradiance pattern of the light receiver [9; 12]. For a flight period equal to 60 days, the mass of the payload with such a STP can reach 2500–2600 kg with a mirror diameter

of over 18–20 m; however, these values are theoretically possible with heating of the gas in the spacecraft system CR above 3200–3400 K, but currently, it does not have reliable experimental confirmation. At more moderate confirmed heating temperatures of the light receiver of about 2800 K, the mass of the PL is up to 2230 kg with a mirror diameter of about 12 meters. In this case, the rational range of the parameter  $\Delta\alpha$  is 0.9–1.1° with the same permissible angular misorientation as the two-stage CATS system.

It could be highlighted here that the operating time of the STP without TES at each apsidal activation is significantly longer compared to the propulsion with TES, which, with much lower thrust, leads to a noticeable increase in gravitational speed losses and an increase in the required amount of fuel. In addition, long-term precision orientation of the CR system to the Sun is complicated by vibrations from the operating propulsion, unlike the STP with TES, when the processes of orientation of the concentrator and propulsion operation are separated.

We could also mention that the energy-mass efficiency of the solar power propulsion system (SPPS) developed at the M.V. Keldysh Research Center and using a graphite TES is limited by the power of the standard solar batteries (SB) of the payload within  $N_{\rm SB} = 10$ –11 kW [24]. If so, the ratio  $Q_{\rm a}/N_{\rm CB} = 15$ –17 MJ/kW. During a 60-day flight to geostationary orbit and afterburning of hydrogen heated in the launch vehicle, an advantage of the STP in the payload mass of up to 100–150 kg is observed, depending on the available power of the SB as part of the payload of the spacecraft with the SPPS.

#### STP with a two-stage CATS system and hydrogen afterburning

The energy-ballistic efficiency of a spacecraft with a STP can in a number of cases be increased by afterburning the hydrogen heated in the TES with a cold oxidizer, which forms fuel vapors with hydrogen with a high stoichiometric ratio of components (for example, oxygen or fluorine) [7; 24–26]. This approach is most advantageous for relatively short-term flights (20–30 days) to high-energy orbits. Reducing the proportion of heated hydrogen allows for a reduction in the size of the CATS system and significantly simplifies its development. In addition, hydrogen afterburning allows the spacecraft to be launched into an intermediate elliptical orbit of 100/300 km in size while the propulsion is running on "cold" components to ensure conditions for the opening of the film concentrator in orbit.

We could consider a flight to GEO in 20–90 days with the afterburning of hydrogen heated in the CATS with cold oxygen. As it has been shown, the energy-ballistic efficiency of a spacecraft with STP is significantly reduced when the flight time is less than 30 days, and an increase in the parameter [p] increases the mass of the payload asymptotically (Fig. 4, 5). However, during the afterburning of hydrogen, the mass of the PN increases in the case of  $T_{\Sigma} = 20-30$  days, characterized by large values of the single thrust impulse  $I_{\text{single}} = 270-390 \text{ kN} \cdot \text{s}$ . The best result in relation to the energy-ballistic efficiency of the spacecraft in this time interval  $T_{\Sigma}$  corresponds to the optimal range of values of the oxidizer excess coefficient  $\alpha = 0.25-0.3$ , at which the mass of the payload is maximum and significantly exceeds that for a single-component propulsion.

The results of calculating the parameters of the STP during hydrogen afterburning for rational values of the coefficient  $\alpha$  are given in Tables 5–10 in relation to the considered range of flight times  $T_{\Sigma}$ . The relevant propulsion parameters are presented that most completely characterize the energy-mass efficiency of a spacecraft with a STP in the task of a flight to GEO.

The results in Tables 5–9 show that the distribution of energy capacities by heating stages in the TES  $Q_{a2}/Q_{a1} = 2.33$  does not change and corresponds to those for a single-component propulsion (Table 4) for any values of the coefficient  $\alpha$  and time  $T_{\Sigma}$ .

The values of  $R_{\text{max}}$  and  $F_{\text{K1}}$  are presented in the tables as important ones, on which, among other things, the radial dimensions of the light receiver-accumulator and the accuracy of the orientation of the CR system to the Sun depend. For the considered CATS system, the angular dynamic orientation  $\beta = \pm 1.64^{\circ}$  remains constant for any values of the flight time and oxidizer excess coefficient. For other

HAM and geometric parameters of the concentrator (angles  $\Theta$  and  $\Delta\alpha$ , as the most significant ones), the permissible misorientation angle  $\beta$  will change.

The radius of the high-temperature stage  $R_1$ , as in the case of a single-component propulsion, is determined from Table 1 in accordance with Tables 5–9, taking into account the afterburning of the component, and determines, together with the value of  $R_{\rm max}$  and the values of  $Q_{\rm al}/Q_{\rm a2}$ , the mass-geometric characteristics of the accumulator stages to determine the isothermal phase-transition processes "melting – crystallization" in it and for optimizing the TES scheme and the CATS system as a whole at subsequent stages of development.

Table 5 Reasonable parameters of a spacecraft with STP ( $T_{\Sigma}$  = 20 days)

α	$I_{\text{specific(eff)}},$	$Q_{\mathrm{a}}$	$Q_{\rm al}/Q_{\rm a2},$	TES	$R_{\max}$ ,	$R_{1,}$	$F_{\kappa 1}$ ,	$N_{\rm r}$ ,	$D_{\kappa 1},$	PL
	m/s	MJ	MJ/MJ	mass,	m	m	m	kW	m	mass, kg
				kg						
0	5326	1977	593/1384	1080	0.350	0.115	9.83	325	22.7	1250
0.1	5366	1257	377/880	688	0.280	0.093	7.84	207	18.1	1526
0.2	5283	944	283/661	516	0.242	0.080	6.80	155	15.7	1590
0.25	5308	832	250/583	456	0.228	0.076	6.39	137	14.7	1650
0.3	5250	756	227/529	413	0.217	0.072	6.08	124	14.1	1640
0.35	5211	691	287/484	378	0.207	0.069	5.82	114	13.4	1620
0.4	5050	653	196/457	357	0.202	0.067	5.65	107	13.1	1550

Reasonable parameters of a spacecraft with STP ( $T_{\Sigma} = 30$  days)

Table 6

Table 7

Table 8

α	$I_{\text{specific(eff)}},$	$Q_{\rm av}$	$Q_{a1}/Q_{a2}$ ,	TES	$R_{\max}$ ,	$R_{1,}$	$F_{\kappa 1}$ ,	$N_{\rm r}$ ,	$D_{\kappa 1}$ ,	PL
	m/s	MJ	MJ/MJ	mass,	m	m	m	kW	m	mass, kg
				kg						
0	5772	1369	410/958	750	0.267	0.089	7.47	187	17.3	1720
0,1	5658	870	261/609	476	0.212	0.071	5.95	119	13.8	1810
0,2	5498	654	196/458	358	0.184	0.061	5.16	90	12.0	1815
0,25	5500	576	173/403	315	0.173	0.057	4.85	79	11.2	1850
0,3	5422	523	157/366	286	0.165	0.055	4.62	73	10.7	1825
0,35	5366	478	143/335	262	0.157	0.052	4.42	66	10.2	1810

# Reasonable parameters of a spacecraft with STP ( $T_{\Sigma} = 45$ days)

α	$I_{ m specific(eff)}, \  m m/s$	Q₃∙ MJ	$Q_{ m al}/Q_{ m a2}, \  m MJ/MJ$	TES mass, kg	R <sub>max</sub> , m	R <sub>1,</sub> m	$F_{\kappa 1}$ , m	N <sub>r</sub> , kW	$D_{\kappa l},$ m	PL mass, kg
0	6091	963	289/674	526	0.209	0.070	5.88	116	13.6	2015
0,1	5857	612	184/429	335	0.167	0.056	4.70	74	10.8	2015
0,2	5642	460	138/322	252	0.145	0.048	4.06	55	9.4	1960
0,3	5535	368	110/258	201	0.130	0.043	3.64	44	8.4	1940

Reasonable parameters of a spacecraft with STP ( $T_{\Sigma} = 60$  days)

α	I <sub>specific(eff)</sub> , m/s	Q <sub>a</sub> , MJ	$Q_{ m al}/Q_{ m a2}, \  m MJ/MJ$	TES mass, kg	R <sub>max</sub> , m	R <sub>1,</sub> m	$F_{\kappa 1},$ m	N <sub>r</sub> , kW	$D_{\kappa 1},$ m	PL mass, kg
0	6286	730	219/511	399	0.174	0.058	4.9	80	11.3	2250
0,1	5975	464	139/325	254	0.139	0.046	3.9	51	9.0	2120
0,2	5727	349	105/244	191	0.120	0.040	3.4	38	7.8	2040
0,25	5601	249	84/195	153	0.107	0.035	3.0	31	6.9	2005

Table 9 Reasonable parameters of a spacecraft with STP ( $T_{\Sigma} = 90$  days)

α	$I_{ m specific(eff)}, \  m m/s$	Q <sub>a</sub> , MJ	$Q_{ m a1}/Q_{ m a2}, \  m MJ/MJ$	TES mass,	R <sub>max</sub> ,	R <sub>1,</sub> m	$F_{\kappa l}$ , m	N <sub>r</sub> , kW	$D_{\kappa 1},$ m	PL mass, kg
				kg						
0	6460	554	166/388	303	0.120	0.040	3.34	38	7.8	2340
0,1	6078	352	106/246	193	0.096	0.029	2.67	24	6.2	2210
0,2	5800	264	79/185	145	0.083	0.027	2.32	18	5.4	2105

As tables 5–9 presents, for a short flight time of 20 days, the mass of the payload increases to the optimal (according to the criterion of the maximum payload mass) value  $\alpha$ = 0.25. The maximum increase in the payload removed during afterburning is 400 kg, reaching a value of 1650 kg with a size of  $D_{\kappa 1}$  = 14.7 m. Reducing the energy capacity of the battery  $Q_a$ , its mass  $M_a$  and the power of the CR system  $N_r$  by 2.37 times, as well as reducing the diameter  $D_{\kappa 1}$  by 1.5 times with a change in  $\alpha$  from 0 to 0.25 significantly simplifies the CATS system. A further increase in the oxidizer excess coefficient leads to a decrease in the payload mass. Here it is necessary to specify, using the "concessions" method, how appropriate it is to slightly reduce the PL mass while simultaneously significantly reducing the size and simplification of the CATS system, taking into account the technical, technological and other aspects of its development.

At  $T_{\Sigma} = 30$  days and the optimal value  $\alpha = 0.25$ , an increase in the mass of the PL by 130 kg is observed with the same rate of decrease in the values  $Q_{\rm a}$ ,  $M_{\rm a}$  and  $N_{\rm r}$ . The results in Tables 6–9 indicate a decrease in the efficiency of afterburning with a longer flight duration.

Since the mass of the payload and the dimensions of the CATS system during a flight time of over 45 days continuously decrease with an increase in the proportion of oxidizer, the choice of the coefficient  $\alpha$  should be made, among other things, taking into account the technical, technological and materials science capabilities of creating the CATS system as a whole, including the issues of cooling the engine afterburning chamber, which are much easier to solve with small values of  $\alpha$ . When making the final choice of the coefficient  $\alpha$ , it is also important to take into account possible chemically non-equilibrium processes during the outflow of combustion products from a chamber with a small critical section of a relatively short nozzle. The choice in this case of a pressure of 1 MPa, which is high enough for this type of propulsion, partially neutralizes the negative impact of non-equilibrium processes on the value of the specific impulse, the clarification of which is usually carried out experimentally. In this case, it could be taken into consideration the thickening of the boundary layer in the nozzle channel, leading to a decrease in the nozzle coefficient  $\phi_{nozzle}$ , which requires its specification.

As Table 10 demonstrates, the ratios  $Q_a/N_r$ ,  $Q_a/M_\kappa$  and  $Q_a/F_\kappa$  increase with increasing flight duration, and for each value of  $T_\Sigma$  these ratios are the same for any values of the oxidizer excess coefficient when choosing rational combinations  $\{I_{\text{single}}, [p]\}$  that best correspond to the given flight time. The  $Q_a/M_a$  ratio showing the TES specific energy capacity does not change for any values of  $T_\Sigma$  and the coefficient  $\alpha$ , and depends, among other things, on the TES design, the efficiency of phase transition processes, and the level of heat loss due to the type of high-temperature thermal insulation.

Relative parameters of the CATS system

Flight time, days

20

30

45

60

90

 $Q_a/N_r$  $Q_a/M_K$  $Q_{\rm a}/F_{\rm K}$  $Q_a/M_a$ MJ/kW MJ/kg  $MJ/m^2$ MJ/kg 6.08 6.095 2.438 1.828 7.30 7.314 2.925 1.828 8.29 8.311 3.324 1.828 9.12 9.142 3.657 1.828 14.60 14.628 5.851 1.828

Table 10

For longer flight period over 45 days, the selection of the  $\alpha$  coefficient requires a compromise between the permissible reduction in the payload mass, on the one hand, and the reduction in the size (simplification) of the CATS system, while observing the conditions for arranging the spacecraft with the SPS inside the payload fairing (PLF). Afterburning at low values of  $\alpha$  is advisable to reduce the volume of the fuel compartment, which, together with the dimensions of the payload, has to correspond to the dimensions of the payload carrier (PLC) of the launch vehicle. For a single-component STP (at  $\alpha=0$ ), the mass of hydrogen is about 3580 kg, which, with a fuel tank volume of about 54 m³ and the diameter of the standard PLF type 14S737 produced by JSC S.A. Lavochkin Association for the Soyuz-2.1b launch vehicle with the Fregat-M upper stage (the volume of the payload zone in the assembly and protection unit (APU) is up to 112 m³ with a circumscribed diameter of 3.44 m and the length of up to 10.4 m), allows to place a spacecraft with a payload the length of which can reach 4-4.4 meters. Afterburning at small values  $\alpha=0$ ,1 reduces the volume of the fuel compartment to 35 m³, which allows it to be located in the PF of a spacecraft with a length increased by more than 2 m.

Obtaining values  $\alpha = 0.25$ –0,3, the volume of the fuel tanks is 22–24 m³, the permissible length of the spacecraft with a payload in this configuration is 7.8–8 m. Using a smaller standard PLF of the PB $\Phi$ -1.750 type with a volume of 90 m³ and a length of 8.45 m (developed by JSC S.A. Lavochkin Association) allows the placement of a spacecraft with a payload of about 6 meters in length, which corresponds to the technology for assembling the PLC. The dimensions of the propulsion with the TES and the orientation system (the dimensions of the film structure of the concentrating system in the container packaging are small and are not considered here) slightly reduce the available length of the spacecraft. Here it is necessary to take into account the dimensions of the payload adapter depending on the layout of the payload carrier (PLC).

For reference, we can indicate the dimensions of the A2100 space platform by Lockheed Martin Commercial Space Systems (USA), with a launch mass of 6741 kg, delivering a payload of 3820 kg to GEO with dimensions of 3×2.5×6 m [27].

#### Conclusion

The article considers a spacecraft for a flight to geostationary orbit with a solar thermal rocket propulsion, made according to a two-stage scheme with a CATS system with a radial-type light receiver-accumulator, containing low-temperature and high-temperature heating stages located in the plane of focus of a mirror solar concentrator of a pseudo-paraboloid shape of a film structure in accordance with the Gaussian distribution diagram of the concentrated radiant flux in the focal light spot. Suitable heat-accumulating materials for the TES stages have been selected. The low-temperature (peripheral ring) TES stage contains energy-intensive lithium hydride (melting point 961 K); the high-temperature (central) stage of the battery contains beryllium oxide, as the most energy-intensive refractory material with a melting point of 2804 K, which ensures a high specific impulse of the engine thrust of 900 s. The issues of choosing the main geometric characteristics of a pseudo-paraboloid solar concentrator are considered. The choice of the accuracy parameter of the concentrator  $\Delta\alpha = 1^{\circ}$  and the half-angle of its aperture  $\Theta = 60^{\circ}$  is substantiated, the radial dimensions of the CATS system are identified.

Rational combinations  $\{I_{\text{single}},[p]\}$  have been defined for the duration of a multi-impulse flight from LEO to GEO from 20 to 90 days, within the limits of a single thrust impulse  $I_{\text{single}} = 90-390 \text{ kN} \cdot \text{s}$  and the parameter  $[p] = M_{\text{K}}/M_{\text{a}} = 0-1-0.3$ . For these values, the main reasonable propulsion characteristics are presented. The obtained results show that the time of launching a payload into geostationary orbit using a STP in 20...90 days is the most preferable between the duration of a flight with chemical engines and an electric rocket flight, including schemes with the spacecraft "orbit raising" into the final orbit.

It has been shown that a STP with a two-stage CATS system allows a significant increase – up to 2.2 times – in the energy-ballistic efficiency of a spacecraft compared to chemical boosters into high orbits such as GEO, reaching values from 1250 to 2320 kg in the considered range of flight times.

When compared with alternative propulsion using concentrated solar energy, the weight savings of the PL can be up to 150–200 kg, depending on the propulsion type.

Compared to upper stages using a combination of high-thrust and low-thrust engines for the final boost of the spacecraft into geostationary orbit (in particular, the upper stage of the Fregat-M type with an electric rocket engine module of the  $C\Pi \Pi$ -140 $\Pi$  size), in the case of using the considered STP, the gain in payload mass exceeds 500–600 kg with the same flight time in the range of  $T_{\Sigma}$  = 60–90 days.

A comparison with the SPPS developed by the Keldysh Research Center shows an advantage in payload weight when using the STP of about 100–150 kg during a 60-day flight, depending on the power of the SPPS standard solar batteries, determined by the required power of the satellite being launched.

Important results also include the justification of the comparatively low rational value of the focusing mirror accuracy (the accuracy parameter  $\Delta\alpha=1^{\circ}$ ) and the reduction of requirements for the orientation of the STP to the Sun (up to the angular misalignment value  $\beta=\pm1,6^{\circ}$  in the dynamic tracking mode) during passive flights along transition trajectories compared to single-stage STP with the same specific impulse of 900 s ( $\Delta\alpha=0.25-0.64^{\circ}$  at  $\beta<0.8-1.2^{\circ}$ ).

It is shown that the relative values  $Q_a/N_r$ ,  $Q_a/M_\kappa$ ,  $Q_a/F_\kappa$ , which characterize the integral indicators of the CATS system, increase with an increase in the time of the PL launch to the GSO, which is caused by a more significant decrease in the size and mass of the concentrator compared to the rate of decrease in the energy capacity of the TES. For different values of the flight time  $T_{\Sigma} = 20$ –90 days, the ratio of the energy capacities of the second (high-temperature) stage  $Q_{a2}$  and the first stage  $Q_{a1}$  is shown, a constituent of  $Q_{a2}/Q_{a1} = 2.33$ , and for a given single thrust impulse  $I_{\text{single}}$ , it does not depend on the parameter [p], as does the total energy capacity of the NES  $Q_a = Q_{a2} + Q_{a2}$  and its mass.

Afterburning of hydrogen heated in the launch vehicle with cold oxygen during a relatively short flight of 20–30 days and an optimal, according to the criterion of maximum mass-ballistic efficiency, value of the oxidizer excess coefficient  $\alpha=0.25$  allows an additional increase in the mass of the payload by 400–150 kg, respectively, a significant reduction in the dimensions of the CATS system and a reduction in the intensity of TES during the launch vehicle discharge. For longer flights, small values of the coefficient  $\alpha$ -0.1 are advisable in order to simplify the CATS system and to match the dimensions of the spacecraft with the dimensions of the payload zone in the payload fairing of the launch vehicle. For any values of the oxidizer excess coefficient for a given flight time, the ratios  $Q_a/N_r$ ,  $Q_a/M_K$ ,  $Q_a/F_K$  and  $Q_a/M_a$  are constant.

The dimensions of the fuel compartment of a spacecraft with STP are significantly reduced by afterburning hydrogen. Calculation of its geometric parameters showed technological compliance with the standard payload fairings of the Soyuz-2.1b launch vehicle.

Therefore, we have demonstrated the possibility of using the Soyuz-2.1b medium-class launch vehicle with the considered solar booster block instead of heavy and expensive Proton-M class launch vehicles with chemical boosters, or interorbital tugs with electric rocket "additional injection" of the payload into high orbits, for the delivery of a wide range of geostationary spacecraft of various classes and purposes, which significantly (over 30–50 %) reduces the cost of launching the payload.

#### Библиографические ссылки

- 1. Kudrin O. I., Finogenov S. L. Solar Heat Rocket Engine with a Heat Accumulator // 44<sup>th</sup> IAF Congress. IAF Paper № 93-R.3.442 (October 16–22, 1993. Graz, Austria).
- 2. McClanahan J. A., Frye P. E. Solar Thermal Propulsion Transfer Stage Design for Near-Term Science Mission Applications // 30<sup>th</sup> AIAA/ASME/SAE/ASEE Joint Propulsion Conference & Exhibit (27–29 June 1994, Indianapolis, IN, USA). AIAA Paper № 94–2999.
  - 3. Левенберг В. Д. Энергетические установки без топлива. Л.: Судостроение, 1987. 104 с.
- 4. Федик И. И., Попов Е. Б. Двигательно-энергетическая установка на солнечных тепловых аккумуляторах // III Междунар. совещания по проблемам энергоаккумулирования и экологии

в машиностроении, энергетике и на транспорте : сб. науч. докладов. М. : ИМАШ РАН, 2002. С. 282–292.

- 5. Грилихес В. А., Матвеев В. М., Полуэктов В. П. Солнечные высокотемпературные источники тепла для космических аппаратов. М.: Машиностроение, 1975. 248 с.
- 6. Финогенов С. Л., Коломенцев А. И. Выбор теплоаккумулирующего материала для солнечного теплового ракетного двигателя. // Вестник СибГАУ. 2016. Том 17, № 1. С. 161–169.
- 7. Финогенов С. Л. Концепция солнечного теплового ракетного двигателя с фазопереходным тепловым аккумулятором и дожиганием водорода фтором // Вестник МГТУ им. Н. Э. Баумана. Сер. Машиностроение. 2018. № 3 (120). С. 44–63. DOI: 10.18698/0236-3941-2018-3-44-63.
- 8. Gilpin M. R, Scharfe D. B., Young M. P., Webb R. Experimental Investigation of Latent Heat Thermal Energy Storage for Bi-Modal Solar Thermal Propulsion // 12<sup>th</sup> International Energy Conversion Engineering Conference (July 28-30, 2014. Cleveland, OH, USA). AIAA Paper № 2014-3832. URL: https://arc.aiaa.org/doi/10.2514/6.2014-3832 (дата обращения: 02 марта 2025).
- 9. Финогенов С. Л., Коломенцев А. И., Назаров В. П. Солнечный тепловой ракетный двигатель с различными типами системы «концентратор–приемник» // Вестник СибГАУ. 2016. Том 17, № 3. С. 738–747.
- 10. Квасников А. В., Кудрин О. И., Мельников М. В. Лаборатория лучистой и солнечной энергии для исследования процессов в высокотемпературных установках // Доклады Всесоюз. конф. по использованию солнечной энергии. М.: Изд. ВНИИТ, 1969. С. 297–343.
- 11. Finogenov S. L., Kudrin O. I., Nickolenko V. V. Solar Thermal Propulsion with the High-Efficient "Absorber-Thermal Storage" System // 48<sup>th</sup> IAF Congress (October 6–10, 1997. Turin, Italy). IAF Paper № 97-S.6.05.
- 12. Кудрин О. И. Солнечные высокотемпературные космические энергодвигательные установки. М.: Машиностроение, 1987. 247 с.
- 13. Engberg R., Lassiter J. Shooting Star Experiment, Pathfinder 2, Inflatable Concentrator Modal Survey in Vacuum Conditions. Dynamics Test Branch // Marshall Space Flight Center. Test Report № SSE-DEVED-97-120 (March, 1998. USA).
- 14. Hawk C. W., Adams A. M. Conceptual Design of a Solar Thermal Upper Stage (STUS) Flight Experiment // 31<sup>st</sup> AIAA/ASME/SAE/ASEE Joint Propulsion Conference & Exhibit (July 10–12, 1995. San Diego, CA, USA). AIAA Paper № 95-2842.
- 15. Engberg R., Lassiter J. Solar Orbital Transfer Vehicle (SOTV) Inflatable Concentrator Modal Survey at SRS Technologies, Inc. // Structural and Dynamics Test Group, Marshall Space Flight Center. (October, 1999. USA). Test Report № SOTV-DEV-ED99-076.
- 16. Вейнберг В. Б. Оптика в установках для использования солнечной энергии. М.: Оборонгиз, 1959. 236 с.
- 17. Федик И. И., Степанов В. С., Якубов В. Я. Аккумуляторы электрической и тепловой энергии на основе фазовых переходов // II Междунар. совещания по проблемам энергоаккумулирования и экологии в машиностроении, энергетике и на транспорте : сб. науч. докладов М. : ИМАШ РАН, 2001. С. 17–25.
- 18. Хохулин В. С., Чумаков В. А. Проектирование космических разгонных блоков с ЖРД. М.: МАИ, 2000. 72 с.
- 19. Сафранович В. Ф., Эмдин Л. М. Маршевые двигатели космических аппаратов. Выбор типа и параметров. М.: Машиностроение, 1980. 240 с.
- 20. Константинов М. С., Мин Тейн. Оптимизация траектории выведения космического аппарата на геостационарную орбиту для транспортной системы с удельным импульсом двигателя 600–900 с. // Труды МАИ. 2017. Вып. № 95. URL: http://trudymai.ru/published.php?ID=84516 (дата обращения: 02 марта 2025).
- 21. О возможности создания электроракетной двигательной установки мощностью 10...30 кВт на базе двухрежимного двигателя СПД-140Д / В. Н. Бойкачев, Ю. Г. Гусев, В. С. Жасан и др. // Космическая техника и технологии. 2014. № 1 (4). С. 48–59.

- 22. Анализ проектно-баллистических характеристик комбинированной схемы выведения космического аппарата на геостационарную орбиту с использованием ракет-носителей среднего класса / А. А. Белик, Ю. Г. Егоров, В. М. Кульков, В. А. Обухов // Авиационно-космическая техника и технология. 2011, № 4 (81). С. 17–21.
- 23. Solar Thermal Propulsion IHPRPT Phase I Demonstration Program / D. M. Lester, G. D. Farmer, M. R. Holmes, Wayne Wong // 43r' AIAA/ASME/ASCE/AHS/ASC Structures (Statement A) Structural Dynamics, and Materials Conference (22-25 April 2002. Denver, CO, USA). Paper AFRL-PR-ED-AB-2002-00.
- 24. Солнечная энергодвигательная установка с электронагревным тепловым аккумулятором и дожиганием рабочего тела / В. Н. Акимов, Н. И. Архангельский, А. С. Коротеев, Е. П. Кузьмин // Полет. 1999. № 2. С. 20–28.
- 25. Kudrin O. I., Finogenov S. L., Nickolenko V. V. Solar Thermal Rocket Engine with Post-Burning: the Possibility of Its Usage in Space // Space Technology. 1996, Vol. 16, No. 1. P. 15–9.
- 26. Финогенов С. Л., Коломенцев А. И. Характеристики солнечного теплового ракетного двигателя с тепловым аккумулятором и дожиганием водорода // Вестник МГТУ им. Н. Э. Баумана. Сер. Машиностроение. 2018. № 4 (121). С. 55–70. DOI: 10.18698/0236-3941-2018-3-55-70.
- 27. Малых Д. А. Использование модульного принципа построения для проектирования различных вариантов исполнения универсальной космической платформы // Вестник Москов. авиац. ин-та. 2023. Т. 30, № 1. С. 64–75. DOI: 10.34759/vst-2023-1-64-75.

#### References

- 1. Kudrin O. I., Finogenov S. L. Solar Heat Rocket Engine with a Heat Accumulator. IAF Paper № 93-R.3.442. 44<sup>th</sup> IAF Congress (October 16-22, 1993. Graz, Austria).
- 2. McClanahan J. A., Frye P. E. Solar Thermal Propulsion Transfer Stage Design for Near-Term Science Mission Applications. 30<sup>th</sup> AIAA/ASME/SAE/ASEE Joint Propulsion Conference & Exhibit. (27-29 June 1994, Indianapolis, IN, USA). AIAA Paper 1994, № 94-2999.
- 3. Levenberg V. D. *Energeticheskie ustanovki bez topliva* [Power plants without fuel]. Leningrad, Sudostroenie Publ., 1987, 104 p.
- 4. Fedik I. I., Popov E. B. [Propulsion Power Plant with solar thermal energy storages]. *Sbornik nauchnih dokladov III Mezhdunarodnogo sovechshania po problemam energoaccumulirovania i ekologii v mashinostroenii, energetike i na transporte* [Proc. III International workshop on the problems of energy accumulating and ecology in engineering, energetics and transportation]. Moscow, IMASH RAS, 2002. P. 282–292 (In Russ.).
- 5. Grilikhes V. A., Matveev V. M., Poluektov V. P. *Solnechnye vysokotemperaturiye istochniki tepla dlya kosmicheskikh apparatov* [Solar high-temperature thermal sources for space vehicles]. Moscow, Mashinostroenie Publ., 1975, 248 p.
- 6. Finogenov S. L., Kolomentsev A. I. [Choice of heat accumulating material for solar thermal propulsion]. *Vestnik SIBGAU*. 2016. Vol. 17, No. 1, P. 161–169 (In Russ.).
- 7. Finogenov S. L. [Conception of solar thermal propulsion with phase-changing thermal energy storage and hydrogen after-burning by fluorine]. *Vestnik MGTU imeni N. E. Baumana. Mashinostroenie*. 2018, No. 3, P. 44–63 (In Russ.). DOI: 10.18698/0236-3941-2018-3-44-63.
- 8. Gilpin M. R, Scharfe D. B., Young M. P., Webb R. Experimental Investigation of Latent Heat Thermal Energy Storage for Bi-Modal Solar Thermal Propulsion. *12<sup>th</sup> International Energy Conversion Engineering Conference* (July 28-30, 2014 Cleveland, OH, USA). AIAA Paper № 2014-3832. Available at: https://arc.aiaa.org/doi/10.2514/6.2014-3832 (accessed 02.03.2025).
- 9. Finogenov S. L., Kolomentsev A. I., Nazarov V. P. [Solar thermal propulsion with different types of concentrator-absorber systems]. *Vestnik SIBGAU*. 2016, Vol. 17, No. 3, P. 738–747 (In Russ.).
- 10. Kvasnikov A. V., Kudrin O. I., Mel'nikov M. V. [Laboratory of radiant and solar energy for investigation of processes in high-temperature installations]. *Doklady vsesoyuznoi konferentsii po is*-

- polzovaniyu solnechnoi energii [Proc. of the USSR conference on solar energy use]. Moscow, VNIIT Publ., 1969, P. 297–343 (In Russ.).
- 11. Finogenov S. L., Kudrin O. I., Nickolenko V. V. [Solar Thermal Propulsion with the High-Efficient "Absorber-Thermal Storage" System]. 48<sup>th</sup> IAF Congress (October 6–10, 1997, Turin, Italy). IAF Paper № 97-S.6.05.
- 12. Kudrin O. I. *Solnechnie vysokotemperaturnye kosmicheskie energodvigatelnye ustanovki* [Solar high-temperature space power-propulsion plants]. Moscow, Mashinostroenie Publ., 1987, 247 p.
- 13. Engberg R., Lassiter J. Shooting Star Experiment, Pathfinder 2, Inflatable Concentrator Modal Survey in Vacuum Conditions. Dynamics Test Branch. *Marshall Space Flight Center* (March, 1998, USA). Test Report № SSE-DEVED97-120.
- 14. Hawk C. W., Adams A. M. Conceptual Design of a Solar Thermal Upper Stage (STUS) Flight Experiment. 31<sup>st</sup> AIAA/ASME/SAE/ASEE Joint Propulsion Conference & Exhibit (July 10-12, 1995, San Diego, CA, USA). AIAA Paper № 95-2842.
- 15. Engberg R., Lassiter J. Solar Orbital Transfer Vehicle (SOTV) Inflatable Concentrator Modal Survey at SRS Technologies, Inc. *Structural and Dynamics Test Group, Marshall Space Flight Center* (October, 1999, USA). Test Report № SOTV-DEV-ED99-076.
- 16. Veinberg V. B. *Optika v ustanovkah dlya ispol'zovniya solnechnoi energii* [Optics in installations for solar energy use]. Moscow, Oborongiz Publ., 1959, 236 p.
- 17. Fedik I. I., Stepanov V. S., Yakubov V. Ya. [Accumulators of electric and heat energy based on phase transitions]. *Sbornik nauchnih dokladov II Mezhdunarodnogo sovechshaniya po problemam energoaccumulirovania i ekologii v mashinostroenii, energetike i na transporte* [Proc. II International workshop on the problems of energy accumulating and ecology in engineering, energetics and transportation]. Moscow, IMASH RAS, 2001, P. 17–25 (In Russ.).
- 18. Khohulin V. S., Chumakov V. A. *Proektirovanie kosmicheskih razgonnyh blokov s ZhRD* [Design of space upper stages with liquid propulsion]. Moscow, MAI Publ., 2000, 72 p.
- 19. Safranovich V. F., Emdin L. M. *Marshevye dvigateli kosmicheskih apparatov. Vybor tipa i parametrov.* [Sustainer engines of space vehicles. Choice of type and parameters]. Moscow, Mashinostroenie Publ., 1980, 240 p.
- 20. Konstantinov M. S., Min Tein [Optimization of spacecraft injection trajectory into geostationary orbit for transportation system with specific impulse of 600–900 sec.]. *Trudy MAI*. 2017, No. 95 (In Russ.). Available at: http://trudymai.ru/published.php?ID=84516 (accessed 02.03.2035).
- 21. Boikachev V. N., Gusev Yu. G., Zhasan V. S. et al. [About the possibility of creation of electric propulsion plant with power of 10...30 kWatt based on two-regime SPD-140D engine]. *Kosmicheskaya tekhnika i tekhnologii*. 2014, No. 1(4). P. 48–59 (In Russ.).
- 22. Belik A. A., Egorov Yu. G., Kul'kov V. M., Obukhov V. A. [Analysis of design-ballistic characteristics of combined scheme of spacecraft injection into geostationary orbit with use of middle-class launchers] (In Russ.). *Aviatsionno-kosmicheskaya tekhnika i tekhnologiya*. 2011, No. 4(81), P. 17–21 (In Russ.).
- 23. Lester D. M., Farmer G. D, Holmes M. R., Wong Wayne. Solar Thermal Propulsion IHPRPT Phase I Demonstration Program. *43r' AIAA/ASME/ASCE/AHS/ASC Structures (Statement A) Structural Dynamics, and Materials Conference* (22–25 April 2002, Denver, CO, USA). Paper AFRL-PR-ED-AB-2002-00.
- 24. Akimov V. N., Arkhangel'skiy N. I., Koroteev A. S., Kuzmin E. P. [Solar power-propulsion plant with electrically-heated thermal energy storage and working medium post-burning]. *Polyet*. 1999, No. 2, P. 20–28 (In Russ.).
- 25. Kudrin O. I., Finogenov S. L., Nickolenko V. V. Solar Thermal Rocket Engine with Post-Burning: the Possibility of Its Usage in Space. *Space Technology*. 1996, Vol. 16, No. 1, P. 15–19.
- 26. Finogenov S. L., Kolomentsev A. I. [Characteristics of solar thermal propulsion with thermal energy storage and hydrogen post-burning]. *Vestnik MGTU imeni N. E. Baumana. Mashinostroenie*. 2018, No. 4(121), P. 55–70 (In Russ.). DOI: 10.18698/0236-3941-2018-3-55-70.

27. Malyh D. A. [Modular Structuring Principle Application for Developing Various Options of the Universal Space Platform Layout]. *Vestnik Moskov. aviats. in-ta.* 2023, Vol. 30, No. 1, P. 64–75. DOI: 10.34759/vst2023-1-64-75.

© Finogenov S. L., Kolomentsev A. I., Nazarov V. P., 2025

**Финогенов Сергей Леонардович** – старший научный сотрудник; Московский авиационный институт (национальный исследовательский университет). E-mail: sfmai2015@mail.ru. https://orcid.org/0009-0004-8901-5010

**Коломенцев Александр Иванович** – кандидат технических наук, профессор; Московский авиационный институт (национальный исследовательский университет). E-mail: aikolomentsev@yandex.ru.

**Назаров Владимир Павлович** – кандидат технических наук, профессор; Сибирский государственный университет науки и технологий имени академика М. Ф. Решетнева. E-mail: nazarov@sibsau.ru.

**Finogenov Sergei Leonardovich** – Senior Researcher; Moscow Aviation Institute (National Research University). E-mail: sfmai2015@mail.ru https://orcid.org/0009-0004-8901-5010

**Kolomentsev Alexander Ivanovich** – Candid. Sc., Professor; Moscow Aviation Institute (National Research University). E-mail: aikolomentsev@yandex.ru.

**Nazarov Vladimir Pavlovich** – Candid. Sc., Professor; Reshetnev Siberian State University of Science and Technology. E-mail: nazarov@sibsau.ru.

Статья поступила в редакцию 01.09.2025; принята к публикации 16.09.2025; опубликована 30.09.2025

The article was submitted 01.09.2025; accepted for publication 16.09.2025; published 30.09.2025

Статья доступна по лицензии Creative Commons Attribution 4.0 The article can be used under the Creative Commons Attribution 4.0 License